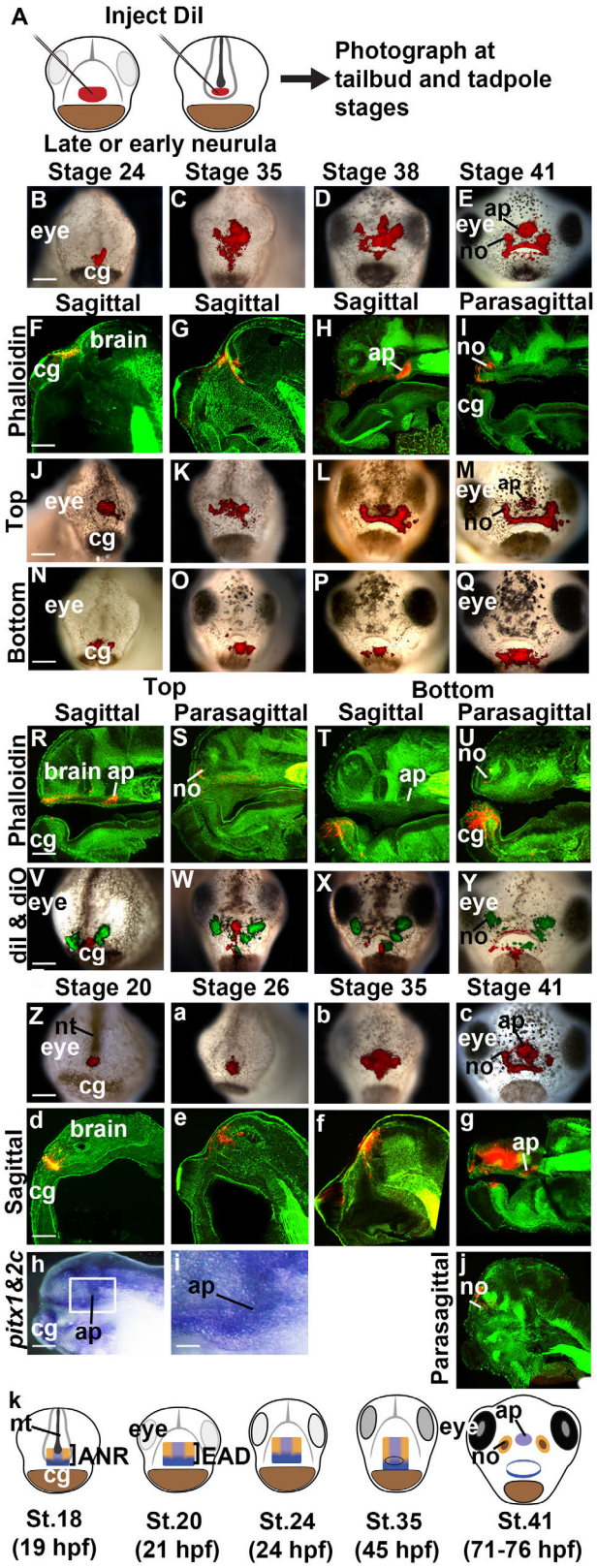
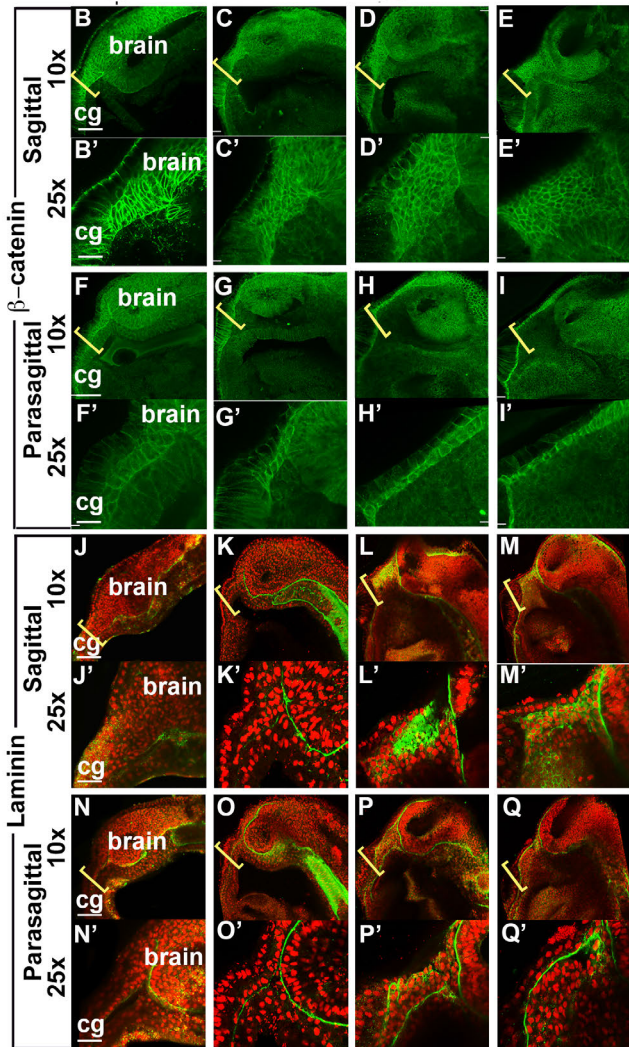
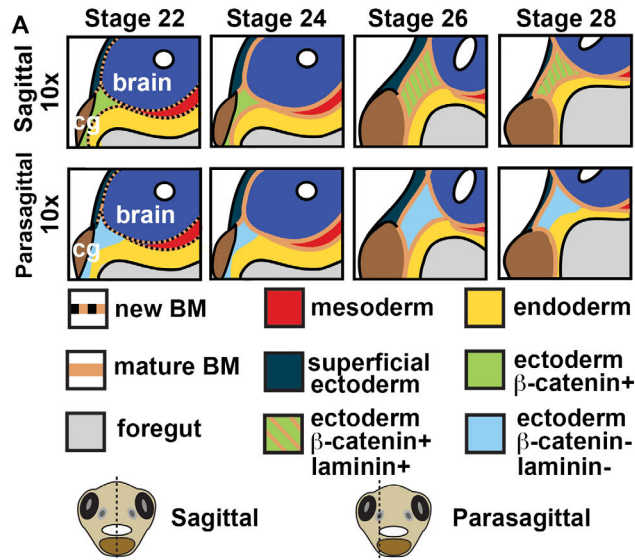


**Formation of a 'pre-mouth array' from
the Extreme Anterior Domain is directed by neural crest and Wnt/PCP signaling**

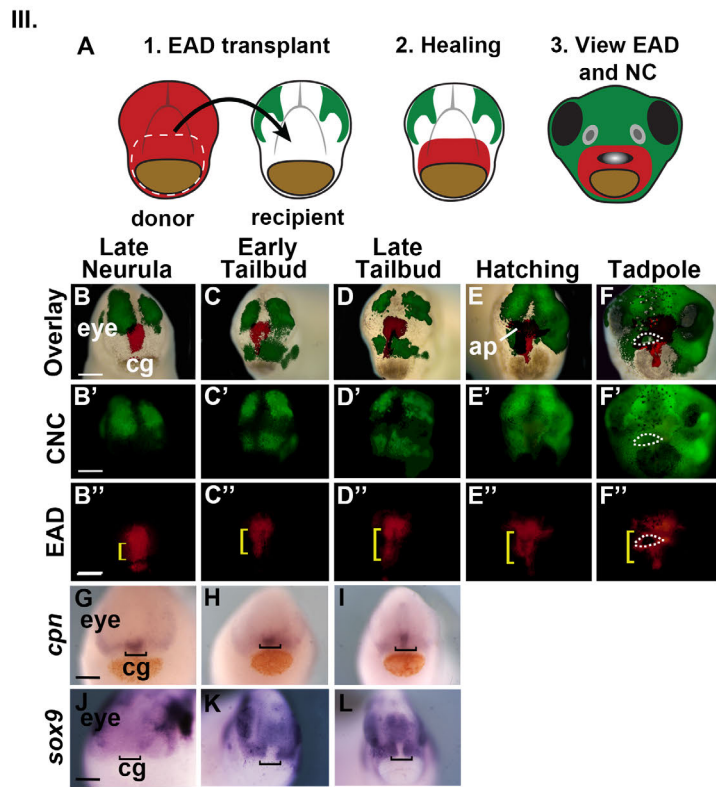
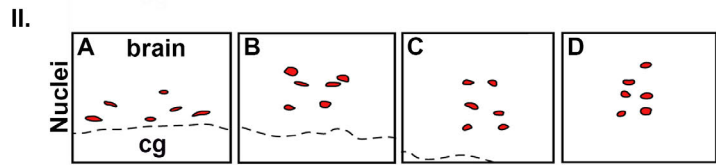
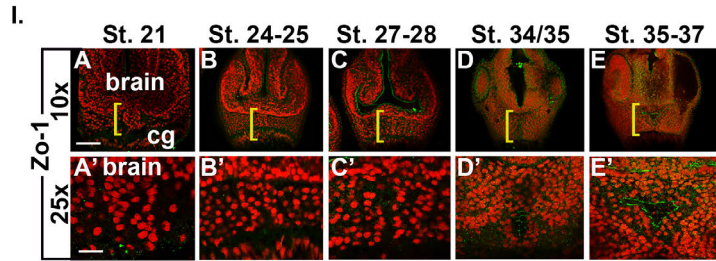
Laura Jacox, Justin Chen, Alyssa Rothman, Hillary Lathrop-Marshall, Hazel Sive.



Supplemental Figure 1: The Extreme Anterior Domain (EAD) ectoderm gives rise to the anterior pituitary (AP), and the lining of the mouth and nostrils, and derives from the anterior neural ridge. Related to Figure 1. (A) Schematic. (B-E) Representative embryo, labeled with DiI in the EAD ectoderm, photographed at four time points (n= 23 from 7 experiments, 78% with label in AP, 100% with label in oral lining, 44% with label in nostril lining). ap, anterior pituitary. cg, cement gland. mo, mouth. Scale bars: 200µm. (F-I) Representative DiI labeled embryo sections at st. 24 (F), st. 35 (G), and st. 41 (H, I) with actin counterstain. Scale bar: 200µm. (J-M) Representative embryo, labeled with DiI in the superior half of the EAD ectoderm, photographed over time (n=12 from 3 experiments, 100% with label in AP, 100% with label in upper oral lining, 0% in lower oral lining, 100% with label in nostril lining). (N-Q) Representative embryo, labeled with DiI in the inferior half of the EAD ectoderm, photographed over time (n=11, 9% with label in AP, 45% with label in upper oral lining, 100% in lower oral lining, 18% with label in nostril lining). (R-U) Representative embryo sections at stage 41, either DiI-labeled in the top (R, S) or bottom (T,U) half of EAD, with actin counterstain. (V-Y) Representative embryo, labeled with DiI in the middle EAD ectoderm and DiO in the lateral EAD ectoderm, photographed over time (n=14 from 3 experiments). (Z-c) Representative embryo labeled with DiI in the anterior neural ridge, photographed at four time points (n= 37 from 8 independent experiments, 73% with label in AP, 100% with label in mouth, 64% with label in nostrils). (d-g, j) Representative DiI labeled embryo sections at stage 20 (d), stage 26 (e), stage 35 (f), and stage 41 (g, j) with actin counterstain. (h, i) In situ hybridization for *pitx1* and *pitx2c*. ap, anterior pituitary. cg, cement gland. Scale bars (B-Z, a-h, j): 200µm. Scale bar (i): 1000µm. (k) Schematic of EAD development. Purple: Future anterior pituitary and lining of upper mouth. Orange: Future nostril lining. Blue: future lining of lower mouth. ANR, anterior neural ridge. EAD, extreme anterior domain. ap, anterior pituitary. cg, cement gland. no, nose. nt, neural tube.



Supplemental Figure 2: Sagittal anatomy of *Xenopus* EAD ectoderm and face between late neurula and swimming tadpole. Related to Figure 1. (A) Schematic of sagittal facial development from stage 22 to 28. (B-I, B'-I') Sagittal and parasagittal sections (3 independent experiments, st. 22, n=12 sagittal, 8 parasag.; st. 24, n=10 sagittal, 6 parasag.; st. 26, n=12 sagittal, 16 parasag.; st. 28, n=12 sagittal, 7 parasag.) with β -catenin immunolabeling. Midline region with bright β -catenin labeling is EAD ectoderm. Bracket: region of 10x image (B-E) enlarged in 25x view (B'-E'). cg, cement gland. Scale bar (10x): 170 μ m. Scale bar (25x): 68 μ m. (J-Q, J'-Q') Sagittal and parasagittal sections (2 independent experiments, st. 22, n=11 sagittal, 8 parasag.; st. 24, n=8 sagittal, 3 parasag.; st. 26, n=17 sagittal, 8 parasag.; st. 28, n=6 sagittal, 3 parasag.) with Laminin (green) immunolabeling with Propidium Iodide (PI) nuclear counterstain (red). Bracket: region of 10x image (F-I) enlarged in 25x view (F'-I'). cg, cement gland. Scale bar (10x): 170 μ m. Scale bar (25x): 68 μ m.



Supplemental Figure 3:

I. The apical polarity marker, *Zo-1*, is localized to apical membrane after pre-mouth array formation, and as oral opening is beginning. Related to Figures 1 and 2. (A-E, A'-E')

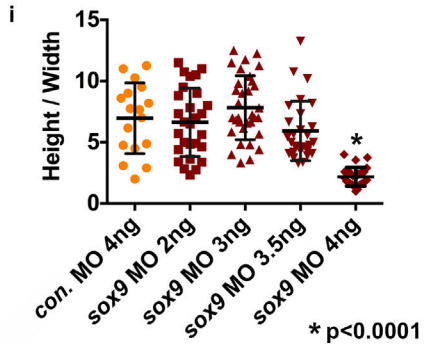
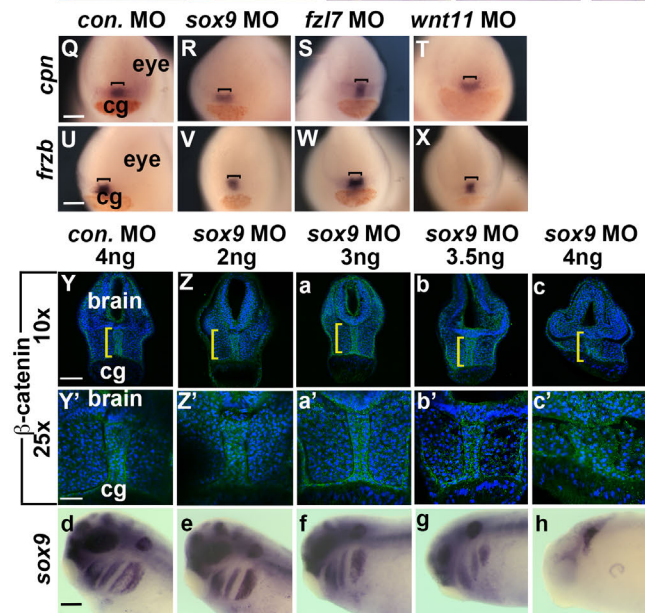
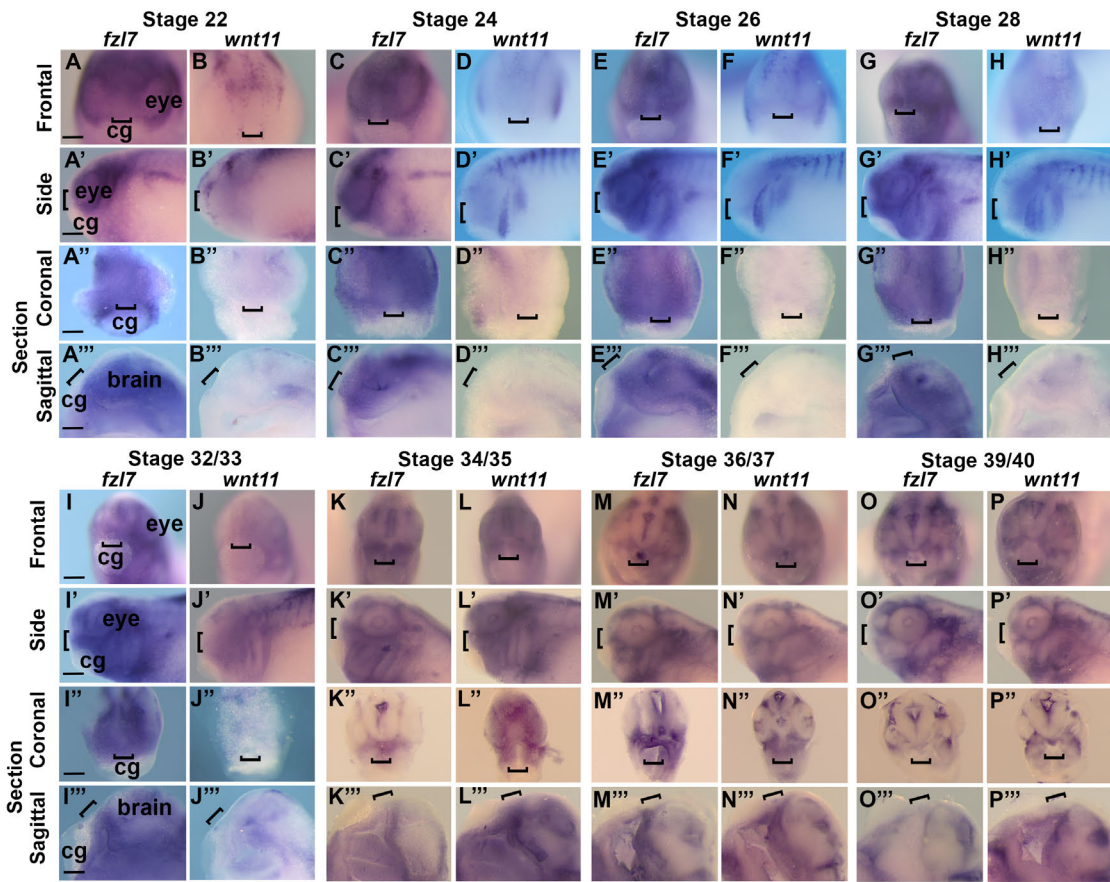
Coronal sections assayed with immunolabeling from late neurula to late hatching. Midline opening with bright labeling at late hatching is part of the EAD ectoderm and the early oral orifice. Representative images shown (st. 21, n=4; st. 24-25, n=3; st. 27-28, n=4; st. 34-37, n=8). Bracket: region of 10x image (A-E) enlarged in 25x view (A'-E'). cg, cement gland. Scale bar (10x): 170 μ m. Scale bar (25x): 68 μ m.

II. Nuclear shape changes indicative of convergent extension. Related to Figure 2. (A-D)

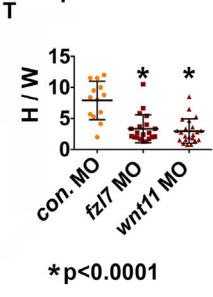
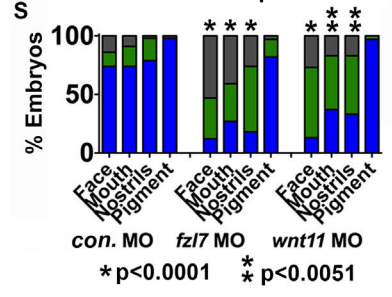
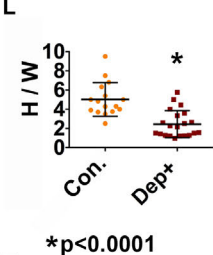
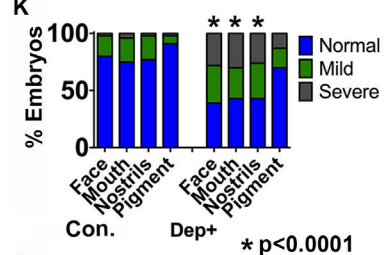
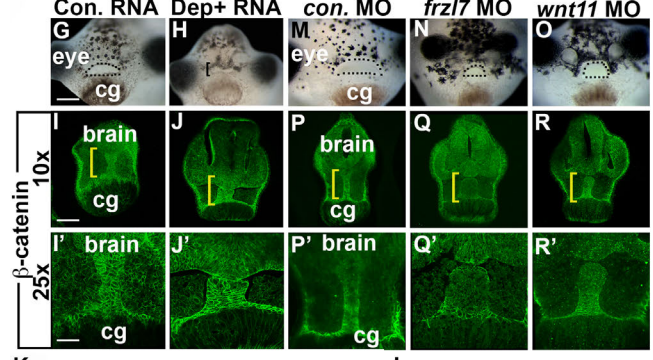
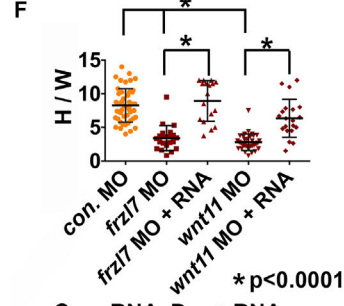
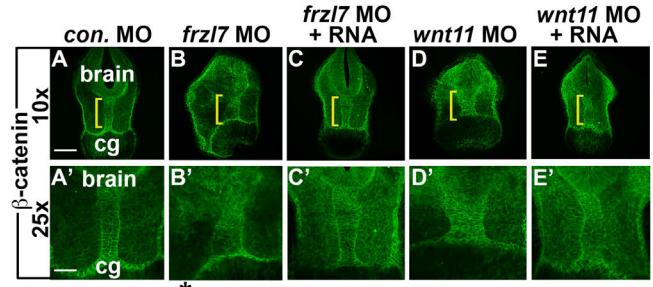
Nuclei of traced cells. Six nuclei shown per stage of EAD cells displayed in Figure 2, A-D''. Dotted line: top of cement gland, cg.

III. EAD ectoderm undergoes convergent extension (CE) as the cranial neural crest (NC) approaches the midline, by live imaging and in situ hybridization. Related to Figure 3. (A)

Experimental schematic. (B-F'') Representative embryo with mGFP labeled NC and mCherry labeled EAD from late neurula (stage 21) to swimming tadpole (stage 40) (3 experiments, n=13). (B-F) Bright field with NC channel (green) and EAD channel (red) overlaid. (B'-F'') NC mGFP (green) channel. (B''-F'') mCherry EAD (red) channel. cg, cement gland. Bracket: region undergoing lengthening and narrowing. Dots surround open mouth. (G-L) In situ hybridization for *cpn* (G-I) and *sox9* (J-L) at late neurula, early and late tailbud. RNA is purple. Cement gland marker (*xcg*) is red. Bracket: presumptive mouth. Scale bars: 200 μ m.

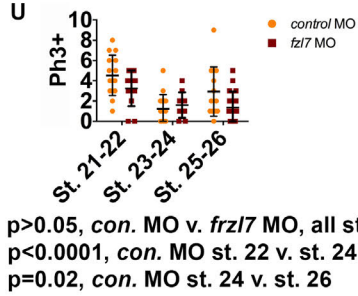
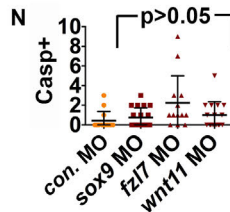
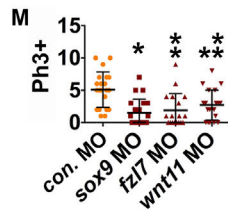
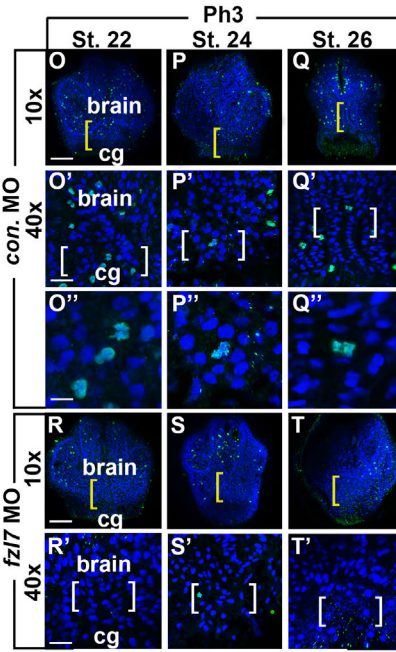
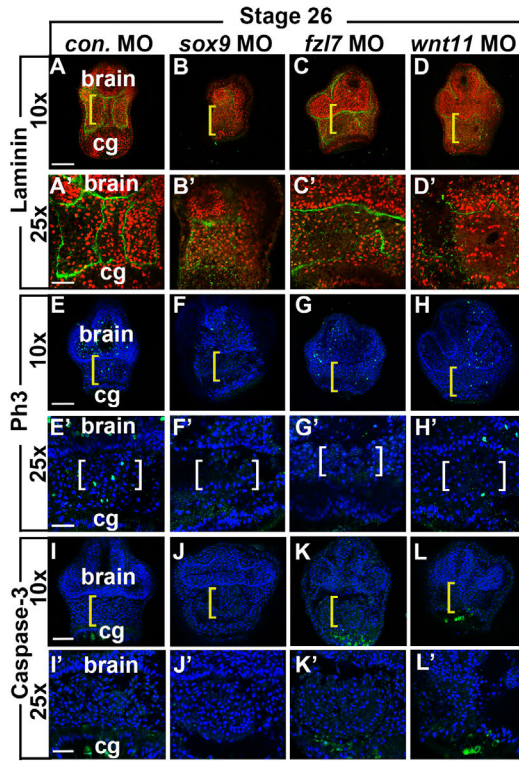


Supplemental Figure 4: *Frizzled7 (fzl7)* and *wnt11* are expressed throughout the head, except *wnt11* expression is low in the midline. Expression of *fzl7* receptor and *wnt11* ligand persist later in craniofacial development (stages 32-40). The EAD is properly specified in *fzl7*, *wnt11*, and *sox9* LOF embryos, as indicated by expression of markers *cpn* and *frzb1*. *sox9* LOF has a threshold effect on convergent extension. Related to Figure 4. (A-P''') In situ hybridization for *fzl7* (A-A''', C-C''', E-E''', G-G''', I-I''', K-K''', M-M''', O-O''') and *wnt11* (B-B''', D-D''', F-F''', H-H''', J-J''', L-L''', N-N''', P-P''') throughout craniofacial development. RNA is purple. Bracket: presumptive mouth. cg, cement gland. Scale bars: 200 μ m. (Q-X) Control, *sox9*, *fzl7*, and *wnt11* LOF embryos at stage 22 express EAD markers, *frzb1* and *xanf1*. Cement gland marker (*xcg*) is red. Scale bar: 200 μ m. (Y-i) Titration of *sox9* morpholino, simulating cranial neural crest titration. (Y-c') Coronal sections, stage 28, assayed in 3 independent experiments. ((Y, Y') control MO 4ng, n=17; (Z, Z') *sox9* MO 2ng, n=28; (a, a') *sox9* MO 3ng, n=33; (b, b') *sox9* MO 3.5ng, n=28; (c, c') *sox9* MO 4g, n=25) with β -catenin immunolabeling and Hoersch nuclear labeling. Midline region with bright β -catenin labeling is EAD ectoderm. Bracket: region of 10x image (Y-c) enlarged in 25x view (Y'-c'). Scale bar (10x): 170 μ m. Scale bar (25x): 68 μ m. (d-h) In situ hybridization for *sox9* at late tailbud. RNA is purple. Scale bar: 200 μ m. (i) Quantification of height over width of EAD (see Methods). P value: unpaired, two-tailed T test. Error bar: standard deviation.



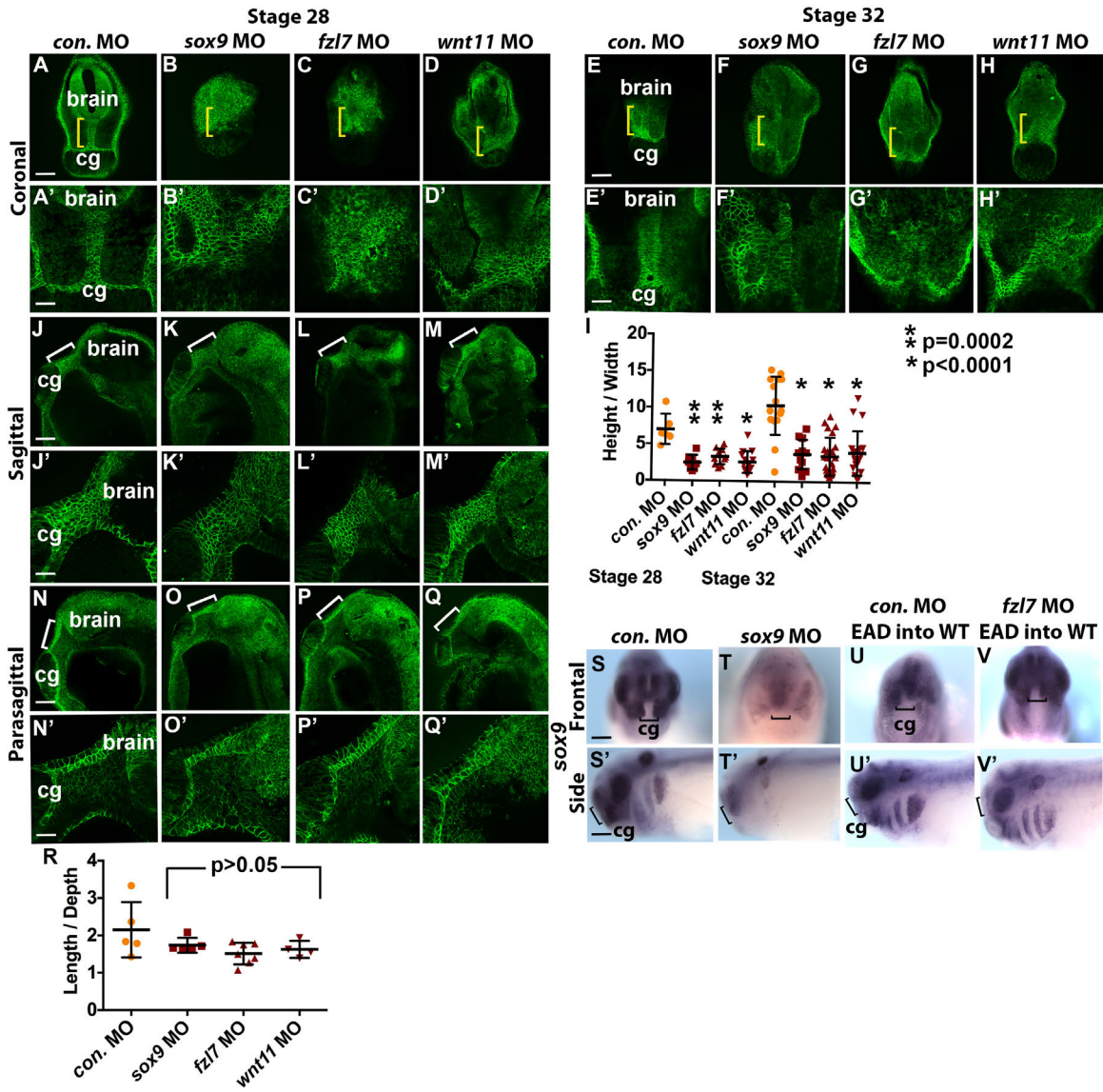
Supplemental Figure 5: *frzl7* and *wnt11* antisense morpholino specificity. Wnt/PCP factors are required for EAD convergent extension and normal mouth formation. Related to Figure 4. (A-F, A'-E') Specificity of *frzl7* and *wnt11* morphant phenotypes was confirmed by rescue of convergent extension at stage 28 with 500ng *frzl7* murine mRNA (C, C') and 700ng *wnt11* murine mRNA (E, E'). Embryos were co-injected with mixture of morpholino and mRNA at the one cell stage. Coronal sections assayed in 2 independent experiments ((A, A') control MO n=47; (B, B') *frzl7* MO n=21; (C, C') *frzl7* MO + RNA, murine *frzl7* mRNA, n=17; (D, D') *wnt11* MO n=33; (E, E') *wnt11* MO + RNA, murine *wnt11* mRNA n=20) with β -catenin immunolabeling. Bracket: region of 10x image (A-E) enlarged in 25x view (A'-E'). (F) Quantification of height over width of EAD (see Methods). P value: unpaired, two-tailed T test. Error bar: standard deviation. (G-H) Frontal view of control and Dep+ RNA injected embryos at swimming tadpole (st. 40) assayed in 3 experiments. ((G) control RNA n=56; (H) Dep+ RNA n=49.) Bracket: unopened mouth. Dots surround open mouths. cg, cement gland. Scale bar: 200 μ m. (I-J') Coronal sections assayed in 3 independent experiments ((I, I') control RNA n=16; (J, J') Dep+ RNA n=21) with β -catenin immunolabeling. Midline region with bright β -catenin labeling is EAD ectoderm. Bracket: region of 10x image (I-J) enlarged in 25x view (I'-J'). (K) Graph depicting percent of embryos, displaying mouth, face, nostrils and pigment formation phenotypes at stage 40 in control and Dep+ embryos. P values: Fisher's exact probability test. (L) Quantification of height over width of EAD (see Methods). P values: unpaired, two-tailed T test. Error bar: standard deviation. (M-O) Frontal view of control MO, *frzl7* MO, and *wnt11* MO injected embryos at swimming tadpole (stage 40) assayed in 3 experiments ((M) control MO n=40; (N) *frzl7* MO n=34; (O) *wnt11* MO n=30). Dots surround open mouths. Scale bar: 200 μ m. (P-R') Coronal sections assayed in 3 independent experiments ((P, P') control MO n=13; (Q, Q') *frzl7* MO n=20; (R, R') *wnt11* MO n=22) with β -catenin immunolabeling. Bracket: region of 10x image (P-R) enlarged in 25x view (P'-R'). Unless otherwise specified: Scale bar (10x): 170 μ m. Scale bar (25x): 68 μ m. Scale bars (40x): 43 μ m. (S) Graph depicting percent of embryos, displaying mouth, face, nostrils and pigment formation phenotypes at stage 40 in control and *sox9* LOF embryos. P values: Fisher's exact probability test. (T) Quantification of height over width of EAD (see Methods). P values: unpaired, two-tailed T test. Error bars: standard deviation.

Results: Embryos injected with mRNA encoding a dominant negative *disheveled* (*dvl*) (Dep+), that primarily targets the Wnt/PCP pathway (Tada and Smith, 2000) failed to undergo EAD elongation and later failed to form an open mouth or nostrils (Figure S7G-L, I'-J'). Further, LOF in either *frzl7* or *wnt11* resulted in diminished EAD elongation and later, tiny, deformed mouths and nostrils that failed to open (Figure S7M-T, P'-R').

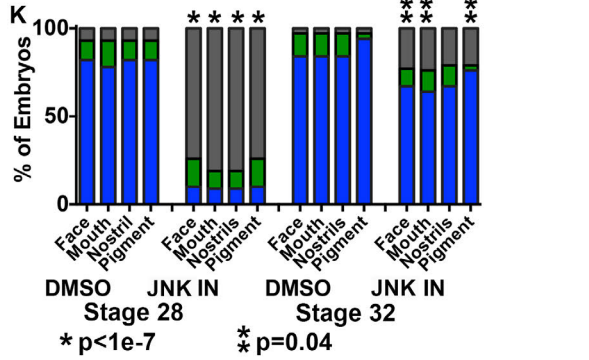
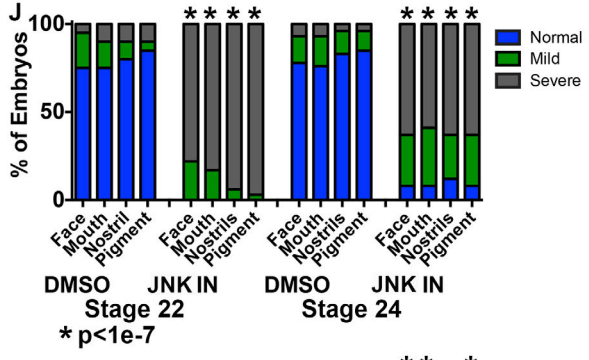
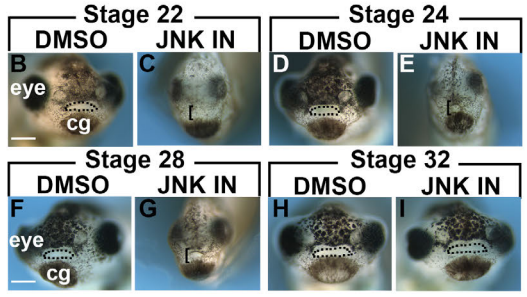
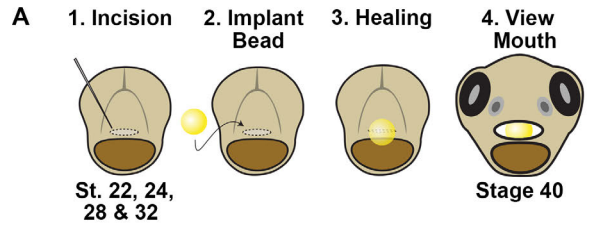


*p < 0.0001 **p = 0.006 ***p = 0.0045

Supplemental Figure 6: Loss of function in Wnt/PCP factors is associated with reduced basement membrane deposition and small changes in cell proliferation and death. Related to Figure 4. (A-D') Coronal sections of control, *sox9*, *fz17*, and *wnt11* LOF embryos assayed with Laminin (green) immunolabeling with Propidium Iodide (PI) nuclear counterstain (red) ((A, A') control MO n=5, 100% normal; (B, B') *sox9* MO n=10, 0% normal; (C, C') *fz17* MO n=14, 14% normal; (D, D') *wnt11* MO n=11, 9% normal). Bracket: region of 10x image (A-D) enlarged in 25x view (A'-D'). (E-H') Coronal sections of control, *sox9*, *fz17*, and *wnt11* LOF embryos assayed with Ph3 (green) immunolabeling with Hoechst nuclear counterstain (blue) ((E, E') control MO n=21; (F, F') *sox9* MO n=21; (G, G') *fz17* MO n=18; (H, H') *wnt11* MO n=20). Yellow bracket: region of 10x image (E-H) enlarged in 25x view (E'-H'). White bracket: region of included Ph3 positive cells. cg, cement gland. (I-L') Coronal sections of stage 24 control, *sox9*, *fz17*, and *wnt11* LOF embryos with cleaved Caspase-3 (green) immunolabeling and Hoechst nuclear counterstain (blue) ((I, I') control MO n=14; (J, J') *sox9* MO n=19; (K, K') *fz17* MO n=13; (L, L') *wnt11* MO n=16). Yellow bracket: region of 10x image (I-L) enlarged in 25x view (I'-L'). cg, cement gland. (M-N) Quantification of Ph3 and cleaved Caspase-3 positive cells in the EAD of LOF embryos. P values: unpaired, two-tailed T test. Error bar: standard deviation. (O-U, O'-T', O''-Q'') Time course of coronal sections of control and *fz17* LOF embryos assayed with Ph3 (green) immunolabeling with Hoechst nuclear counterstain (blue) (2 independent experiments; (O-O'') control MO st. 22 n=15; (P-P'') control MO st. 24 n=17; (Q-Q'') control MO st. 26 n=14; (R, R') *fz17* MO st. 22 n=12; (S, S') *fz17* MO st. 24 n=10; (T, T') *fz17* MO st. 26 n=17). Yellow bracket: region of 10x image (O-T) enlarged in 25x view (O'-T'). White brackets: region of 25x image (O'-Q'') enlarged in 40x view (O''-Q''). White brackets: region of included Ph3 positive cells. cg, cement gland. Scale bar (10x): 170µm. Scale bar (25x): 68µm. Scale bars (40x): 43µm. (U) Quantification of Ph3 positive cells in the EAD of control and *fz17* LOF embryos from stage 22 to 26. P values: unpaired, two-tailed T test. Error bars: standard deviation.



Supplemental Figure 7: *sox9*, *frizzled7* (*fzl7*), and *wnt11* LOF embryos fail to recover from convergent extension defects and sagittal views demonstrate a lower length to depth ratio. Related to Figure 4. (A-H, A'-H') Control, *sox9*, *fzl7*, and *wnt11* LOF embryos at stages 28 and 32. (A, A', E, E') Control LOF embryos (stage 28 n=6; stage 32 n=15). (B, B', F, F') *sox9* LOF embryos (stage 28 n=8; stage 32 n=12) (C, C', G, G') *fzl7* LOF embryos (stage 28 n=11; stage 32 n=24). (D, D', H, H') *wnt11* LOF embryos (stage 28 n=14; stage 32 n=19). Bracket: region of 10x image (A-H) enlarged in 25x view (A'-H'). cg, cement gland. Scale bar (10x): 170 μ m. Scale bar (25x): 68 μ m. (I) Quantification of height over width of EAD ectoderm (see Methods). P values: unpaired, two-tailed T test. Error bar: standard deviation. (J-Q') Sagittal and parasagittal sections of stage 28 control, *sox9*, *fzl7*, and *wnt11* LOF embryos with β -catenin immunolabeling. Midline region with bright β -catenin labeling is EAD ectoderm. Representative images shown (control n=5, *sox9* LOF n=5, *fzl7* LOF n=7, and *wnt11* LOF n=4). Bracket: region of 10x image (J-Q) enlarged in 25x view (J'-Q'). cg, cement gland. Scale bar (10x): 170 μ m. Scale bar (25x): 68 μ m. (R) Quantification of length over depth of EAD (see Methods). P values: unpaired, two-tailed T test. Error bar: standard deviation. (S-T') In situ hybridization of *sox9* in control and *sox9* LOF embryos assayed in 2 experiments (n=14). (S-T) frontal. (S'-T') side view. Bracket: EAD ectoderm. Scale bar: 200 μ m. (U-V') In situ hybridization of *sox9* in control and *fzl7* LOF EAD transplants assayed in 2 experiments (n=16). (U-V) frontal. (U'-V') side view. Bracket: EAD ectoderm. Scale bar: 200 μ m.



Supplemental Figure 8: Inhibition of GTPase JNK throughout convergent extension is associated with aberrant mouth formation. Related to Figure 5. (A) Experimental schematic of inhibitor loaded bead implantation in the presumptive mouth, EAD region, at four time points. Time points include: stage 22- convergent extension beginning, stage 24- convergent extension occurring, stage 28- convergent extension concluding, stage 32- oral invagination, stomodeum, forming. (B-I) Frontal view of swimming tadpole (stage 40) embryos with inhibitor loaded beads implanted in presumptive mouths, assayed in 3 experiments. ((B) control DMSO st. 22 n=20; (C) JNK inhibitor st. 22 n=18; (D) control DMSO st. 24 n=46; (E) JNK inhibitor st. 24 n=24; (F) control DMSO st. 28 n=27; (G) JNK inhibitor st. 28 n=31; (H) control DMSO st. 32 n=31; (I) JNK inhibitor st. 32 n=42.) Bracket: unopened mouth. Dots surround open mouths. cg, cement gland. Scale bars: 200 μ m. (J, K) Graphs depicting percentage of embryos, displaying mouth, face, nostrils and pigment formation phenotypes at stage 40. P values: Fisher's exact probability test.

Supplemental Movie 1: Sagittal anatomy of *Xenopus* EAD ectoderm and face at late tailbud. Related to Figure 1. Representative sagittal sections with Laminin immunolabeling, demonstrating basement membrane (BM) boundaries of the EAD ectoderm. BM lies above the EAD ectoderm (abutting the epidermal ectoderm and brain), below it (abutting the pharyngeal endoderm) and on either side (abutting the NC). In the first embryo, sections progress from a region lateral to the EAD, through the BM wall and into the EAD ectoderm. In the second embryo, sections demonstrate the BM walls of the EAD, following removal of EAD ectodermal cells. The 3D reconstruction highlights the rectangular prism shape of the BM boundaries.

Supplemental Movie 2: Coronal anatomy of *Xenopus* pre-mouth array ectoderm between late neurula and swimming tadpole. Related to Figure 1. Representative coronal sections with β -catenin immunolabeling. Claymation demonstrating morphogenesis of EAD pre-mouth array ectoderm, culminating in mouth opening.